# Lattice Monte Carlo study of clustering transitions in soft matter systems

Bianca M. Mladek[1, 2]

[1]*Center for Computational Materials Science and Institut für Theoretische Physik, Technische Universität Wien, Wiedner Hauptstraße 8-10, A-1040 Wien, Austria*
[2]*SARA Reken- en Netwerkdiensten, Kruislaan 415, 1098SJ Amsterdam, The Netherlands*

(Dated: May 25, 2006)

According to the present state of the art, soft matter systems with purely repulsive interactions are supposed to show under compression two different scenarios: either a re-entrant melting transition or the formation of ordered structures of clusters. In the latter scenario, it is apparently energetically most favourable that the particles form clumps of overlapping particles, so-called clusters, which themselves arrange on a regular lattice. To accurately determine the phase behaviour of the system, fast and efficient Monte Carlo simulation techniques are required. Technical problems that arise in the simulations of the system during the process of cluster formation and during the freezing transition have to be overcome. The simulation results are complemented by density-functional theory calculations that confirm the occurrence of first-order phase transitions into cluster crystals upon compression.

## I. INTRODUCTION

During the past twenty years soft matter has become a rapidly developing field of interest with a highly interdisciplinary character, bringing together physicists, chemists, and biologists in their investigations. One obvious reason for these activities is certainly the fact that soft matter is omnipresent in our daily life: from DNA to proteins, from clay to plastics, from mayonnaise to blood - soft matter is what we are made of and what we use in countless everyday applications. Another reason is the fact that many soft matter systems are of technological relevance, for instance in the biotechnological, food, or pharmaceutical industries. And finally, there is the academic interest in exploring hitherto unknown scenarios for the emergence of mesoscopic structures in novel, composite systems.

Focusing on physics and physical chemistry, soft matter offers ideal possibilities for close cooperations between experimentalists and theoreticians: the ability to control the architecture and chemical nature of the constituting entities of the soft systems, combined with the flexibility in influencing the properties of the solvent in which they are immersed, give rise to an unprecedented freedom in tuning the effective interactions between such entities and opens up the possibility to steer the macroscopic properties of the system [1, 2].

Typical soft matter systems that we deal with are dispersions of mesoscopic particles (with sizes ranging from nm to µm) immersed in a microscopic solvent. These mesoscopic particles are themselves aggregates of several thousands of atoms or molecules arranged in complex, but quite loose internal structures. On a macroscopic level, distinct differences with respect to atomic systems are observed: soft matter materials show a sensitive reaction to mechanical deformations, which is several orders of magnitude higher than in atomic systems and a higher viscosity than atomic liquids, being in some cases even unable to flow. Also on the microscopic level obvious differences can easily be identified: in atomic systems the interaction potentials are essentially fixed by the electronic properties [3]. In soft matter systems, on the other hand, the huge number of degrees of freedom of the constituent particles and of the solvent has to be traced out by suitable methods [1], leading to effective potentials between the mesoscopic particles (see Fig. 1). Those potentials depend both on the architecture and composition of these aggregates, as well as on the nature of the solvent where they are immersed in, which permits to modify them in a well-defined manner. Consequently a large variety of effective interparticle potentials can be obtained, that range from strongly repulsive, hard sphere like interactions to so-called soft potentials that either diverge weakly at the origin (like for star polymers [4]) or even remain finite at short distances (like for isolated non-intersecting polymer chains or dendritic macromolecules [5, 6]). This corresponds to the fact that due to their loose structure the mesoscopic particles are now able to mutually overlap or even to intertwine.

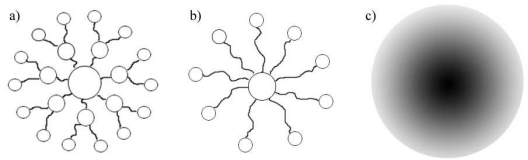


FIG. 1: a) Schematic representation of a dendrimer, which is a synthesised macromolecule built by branched units. b) Schematic representation of a star polymer. c) Schematic representation of an 'effective' particle where all degrees of freedom apart from the center of mass location have been traced out and which interacts with other particles via a soft potential.

In our investigations we will concentrate on soft matter systems for which effective potentials are purely repulsive and remain finite at short distances. Accurate theoretical concepts [1] as well as advanced numerical simulation techniques [7] were developed to describe the properties

of such systems even on a quantitative level. Up to now, two different scenarios were identified [8] that describe how these systems will behave upon compression: either re-entrant melting will take place or they will freeze at all temperatures into crystals where lattice sites are multiply taken, i.e. each lattice site is occupied by a cluster of particles. The first phenomenon has been verified for several soft matter systems such as star polymers, microgels or the before mentioned dendrimers [6, 9]: The systems first freeze, but upon further compression, it becomes energetically more favourable for them to re-melt, i.e., they again form a disordered structure. Several of these liquid-solid-liquid transitions can take place upon compressing the system, but the stable phase at high densities will be the fluid one. In the clustering scenario [10], on the other hand, particles start to sit very close or even on top of each other, i.e., they form clusters which themselves arrange in regular structures. This might seem counter-intuitive at first, as it occurs at the complete absence of attraction, and it demonstrates how fundamentally different soft matter realizes favourable arrangements compared to systems with harshly repulsive potentials.

Compared to the re-entrant melting scenario, little has been done up to now for the clustering transition. This is mostly due to the fact that techniques developed to describe atomic systems or systems that show re-entrant melting break down as soon as clustering sets in and without being generalised, they are not able to describe this phenomenon. Thus, the aim of my project was to develop techniques that give further and quantitative insight into clustering.

This paper is organised as follows: In Sec. II we introduce the model system under study. Sec. III focuses on conventional simulation techniques and their intrinsic problems, while in Sec. IV we present techniques designed to overcome those problems. With these new methods at hand, we analyse the system in Sec. V and draw our conclusions in Sec. VI.

## II. THE SYSTEM

We propose a model system which we call generalised exponential model of index $n$ (GEM-$n$). Its interaction is given by

$$\Phi(r) = \varepsilon \exp[-(r/\sigma)^n]. \quad (1)$$

$\varepsilon$ and $\sigma$ are energy and length parameters, $r$ is the distance between the centers of two particles and $n$ is an arbitrary positive number. We also introduce the number density $\varrho$ and temperature $T$, as well as $\beta = (k_\mathrm{B}T)^{-1}$, with $k_\mathrm{B}$ being Boltzmann's constant.

A criterion put forward in [8] that determines whether a system with a given bounded (i.e., finite) and entirely repulsive potential will show re-entrant melting or will freeze into cluster crystals is based on whether its Fourier transform is positive semidefinite for all wave vectors or not. For the GEM-$n$, it can be shown that for $n \leq 2$, it will show re-entrant melting, while for $n > 2$, clustering will take place at all temperatures [11].

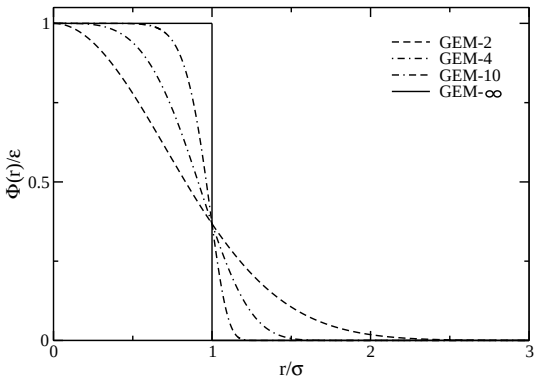


FIG. 2: The potential of the GEM-$n$ for $n$ = 2, 4, 10, and $\infty$. The GEM-2 is equivalent to the Gaussian core model, the GEM-$\infty$ to the penetrable sphere model.

As an example of the clustering phenomenon, we show two simulation snapshots in Fig. 3. At a low density (left panel), the system is apparently in the fluid phase, formed by isolated particles as well as small clusters, whereas at a higher density (right panel), clusters of particles whose crystalline arrangement is clearly visible have formed upon compression.

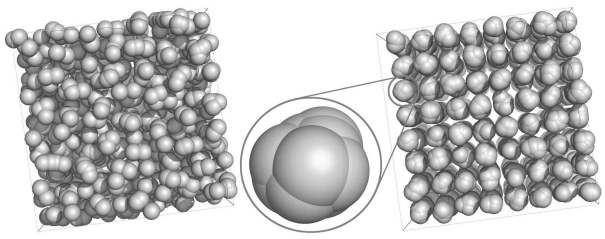

FIG. 3: Two simulation snapshots of a GEM-4 system for $\beta\varepsilon = 2.5$ and $\varrho\sigma^3 = 2.5$ (left) and 7 (right). The inset in the center shows a close up of one cluster. Particle diameters are not drawn to scale.

Suitably tailored dendrimers that have been assembled in a computer simulation show evidence for a GEM-$n$-type of effective interaction with $n > 2$. Thus, our model is able to reflect the properties of realistic systems [12].

## III. MONTE CARLO SIMULATIONS

Monte Carlo (MC) methods are algorithms that use random numbers to solve numerical problems which can be described by a stochastic process. One major field of application of MC methods can be found in statistical mechanics, where these methods are used to determine the thermodynamic or structural properties of a given system. So let us assume that we study a system of $N$

particles interacting via a given potential $\Phi(r)$ and confined in a cubic box of box-length $L$ (i.e., at fixed volume) and at fixed temperature $T$. At first, the particles are placed in an arbitrary configuration within the box. Then, each of the particles is moved randomly according to

$$\mathbf{r}_i \rightarrow \mathbf{r}_i + \Delta\boldsymbol{\xi}_i \qquad i = 1, ..., N \tag{2}$$

where $\mathbf{r}_i$ are the coordinates of particle $i$, $\Delta$ is the maximum allowed displacement, which is arbitrary within the constraint $\Delta < \frac{L}{2}$, and the $\boldsymbol{\xi}_i$ are vectors that have random numbers between $-1$ and 1 as components. After the move, the particle is equally likely to be anywhere in a cube of side $2\Delta$ centred around its original position. To decide whether such a move will be accepted or not, the change in potential energy, $\Delta U = U_{\text{new}} - U_{\text{old}}$, of the system caused by the displacement of the particle is calculated, where $U = \sum_{i<j} \Phi(\mathbf{r}_{ij})$ is the potential energy for a confirmation and $r_{ij}$ is the vector connecting particles $i$ and $j$. If $\Delta U < 0$, i.e., if the energy of the system is now lower than before, the trial move is accepted and the particle is shifted to its new coordinates. On the other hand, if $\Delta U > 0$, the trial move is allowed with a probability of $\exp(-\beta\Delta U)$. Disregarding if the new configuration has been accepted or not, i.e. the system is still in the old configuration, we consider it to be in a new configuration for the purpose of taking ensemble averages. After this trial move, the procedure is repeated with another, randomly chosen particle and so forth, generating a *random walk* through the space of all possible configurations.

This algorithm, which is called "Metropolis MC", satisfies the condition of "detailed balance" [7], which ensures that the MC algorithm generates a new state according to the equilibrium probability distribution function of the ensembles. This condition, if fulfilled, ensures that on average the system should go from a given old state to a new state just as often as from the new state to the old one.

In this conventional MC simulation algorithm, the determination of the potential energy is the most time-consuming part. In a system of $N$ particles interacting with each other via a pairwise additive potential $\Phi(r)$, $N(N-1)/2$ distances and interactions have to be calculated. Thus, the computing time needed to evaluate the energy scales as $N^2$.

In simulations of atomic or soft systems that show reentrant melting, already low particle numbers of around 500 correspond to sufficiently large simulation boxes to provide reliable results. In case of the clustering scenario, however, particles tend to form clumps and to overlap to a large extend. Thus, significantly more particles are needed to simulate systems of comparable size. In case of the conventional MC simulations described in this section, at least 5000 or even more particles are needed. For such a large number of particles, simulations can take several weeks per point in the $T$-$\varrho$ space of states.

## IV. SPEEDING UP THE SIMULATIONS

In order to make MC simulations of clustering systems feasible, we need to considerably speed up the simulations. In this effort, we implement a specially designed, discretised MC technique, the so-called Lattice Monte Carlo (LMC), proposed by Panagiotopoulos [13], and on the other hand, we use the standard technique of the cell list method (cf. Sec. IV B).

### A. Lattice Monte Carlo

#### 1. Central idea

The central idea of LMC is illustrated in Fig. 4. Consider a particle with a characteristic diameter $\sigma$. Introducing the lattice discretisation parameter $\zeta$ we construct a series of lattice models, where we restrict allowed particle positions to be on a simple cubic grid of characteristic spacing $l$. $\zeta$ is determined by the amount of grid sites per particle diameter

$$\zeta = \frac{\sigma}{l}, \tag{3}$$

and it controls how closely the lattice model mimics the continuum behaviour. It can easily be seen from the upper panels of Fig. 4, that a small value of $\zeta$ will have a strong effect on the structural as well as the thermodynamic properties of the system. To demonstrate this let us consider (as this is done in our specific case) a system that shows clustering upon compression, where particles tend to sit very close or even on top of each other. Then if $\zeta$ is very low, there are only few grid points available for further particles to be positioned close to the center of a tagged particle. However, as $\zeta$ increases, i.e. as the grid becomes finer, more and more grid points are accessible within the diameter of the tagged particle and the features of clustering can be represented in an appropriate way. Thus, artefacts due to the lattice discretisation decrease as $\zeta$ is increased. For our implementation of the LMC method, we again use a cubic box of box-length $L$. The box is discretised via a grid using $2^b$ (i.e. $b$ bits) of possible positions in each dimension. Thus, the discretisation parameter now takes the form

$$\zeta = \frac{2^b}{L}. \tag{4}$$

It should be noted that the product $L \times \zeta$ has to be an integer (even though $L$ and $\zeta$ can take any real value individually) so that we can use periodic boundary conditions within the LMC simulations.

Due to the grid there is now only a finite number of possible distances between two particles. Assuming that the interaction potential between any two sites is translationally invariant, we can write the potential energy as

$$U = \sum_{i<j} \Phi(\mathbf{r_{ij}}) = \sum_{i<j} \Phi(r_{ij}), \tag{5}$$

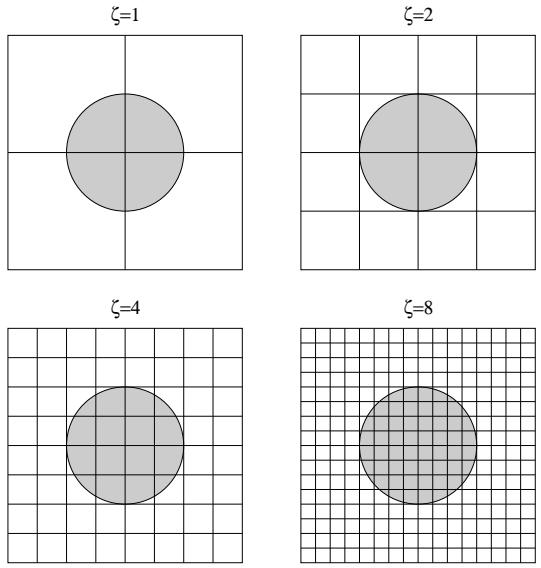


FIG. 4: Schematic representation of the refinement process of the lattice model with increasing lattice discretisation parameter $\zeta = 1$, 2, 4 and 8 as described in the text. For clarity, a two dimensional system is shown, but the generalisation to three dimensions is straight forward. Note that the number of grid points within the tagged particle (grey sphere) grows as $\zeta$ increases.

where $\mathbf{r_{ij}}$ is the vector connecting sites $i$ and $j$ and its modulus $r_{ij}$ is given by

$$r_{ij} = \sqrt{(x_j - x_i)^2 + (y_j - y_i)^2 + (z_j - z_i)^2}. \qquad (6)$$

Now, $x_k$, $y_k$, and $z_k$ are integers between 0 and $2^b - 1$, $k = i, j$. Since for a LMC simulation the possible distances $r_{ij}$ are limited to a finite number, it is obvious from Eq. (5) that we only need to calculate interactions at all possible distances *once* at the beginning of the simulation, storing them in an array of length $3\left[2^{2(b-1)}\right] + 1$.

Depending on the functions involved in the evaluations of the potential studied, the LMC method allows for a speed up of around 20 compared to the conventional MC scheme. This considerable reduction in computational time can be traced back to the elimination of the minimum distance image convention and the time consuming evaluations of the potential for every pair of interacting particles. If - as in our case - we use a power of 2 as number of grid sites per dimension, a further speed up can be achieved since periodic boundary conditions reduce to a bit operation: as soon as a particle leaves the box, its coordinates will need more than $b$ bits to be represented as a binary number on the computer. Trimming to the lowest $b$ bits, periodic boundary conditions are automatically fulfilled (see Fig. 5). Since computers use the binary representation of numbers, bit operations can be performed extremely fast.

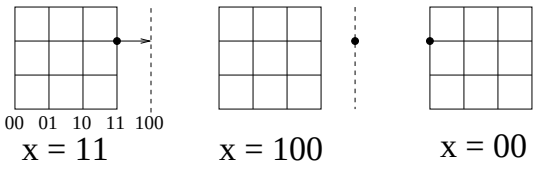


FIG. 5: Schematic representation of periodic boundary conditions within the LMC simulations using a discretisation of 2 bits per direction. Before the move (left panel), the particle has the $x$-coordinate x=11 in the binary representation. During the move (central panel), the particle leaves the simulation box. To store the new coordinates (x=100) on the computer, 3 bits are needed. Trimming the coordinates back to 2 bits leads to the correct new coordinates within the box (right panel).

### *2. The radial distribution function in LMC*

In liquid state theory [14], the radial distribution function (RDF) is defined as

$$g(\mathbf{r}) = \frac{1}{\varrho\sigma^3 N} \left\langle \sum_{i=1}^{N} \sum_{j=1, j\neq i}^{N} \delta(\mathbf{r} - \mathbf{r}_{ij}) \right\rangle \qquad (7)$$

where $\langle \ldots \rangle$ denotes an ensemble average. The RDF gives a measure of the probability to find a particle at a certain distance from a given particle compared to the same probability in an ideal gas. For isotropic and homogeneous systems, the RDF is independent of the direction and only depends on the distance $r = |\mathbf{r}|$ between the particles.

In conventional MC simulations, the RDF is obtained from a histogram of the observed particle distances, which, at the end of the simulation, has to be scaled according to the pre-factors in Eq. (7) and taking under consideration the volumes of the spherical shells in which we measured the histogram. The bin size $\Delta r$ of the histogram (i.e. the thickness of the spherical shells) has to be chosen sufficiently small to capture all correlations, but large enough to minimise the statistical error per bin. By measuring a histogram, the RDF is averaged per bin which leads to a significant error at small distances since the volume of the spherical shells over which we average is small.

In LMC simulations, this problem is even more serious due to the fact that there are only few grid points at small distances and that the number of available grid points is not exactly proportional to the volume of a corresponding spherical shell. Fortunately, one can measure the RDF in a different, and more efficient and accurate way in LMC simulations by using Eq. (7) directly, which can be done because particles can only be located at discrete distances and since the number of possible particle separations is finite. In the final result, one then has to take into account how many times each of the given distances can occur.

The advantage of this approach is that the RDF measured in LMC contains valuable additional information on the state of the system compared to the RDFs measured in conventional MC. In the fluid phase, particles can - in principle - have any distance to each other. During the course of the simulation, all possible distances on the grid will be visited, giving the impression that the RDF is a continuous curve. If, on the other hand, the system is in the solid phase, only a few, certain distances between two particles will be possible (due to thermal vibrations). In this case, the RDF will show pronounced peaks at the corresponding distances (see Fig. 6). By averaging, the RDF can be smoothed and reduced to the form usually obtained by conventional MC.

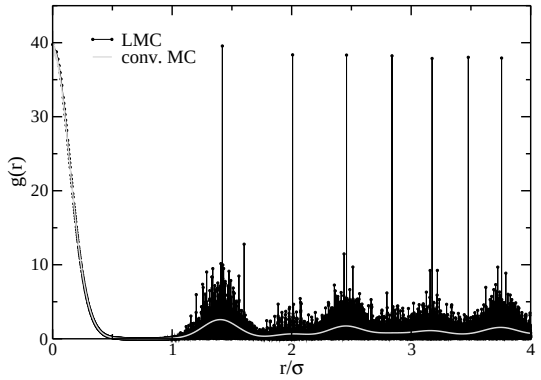


FIG. 6: Simulation results for a GEM-4 at $\beta\varepsilon = 1$ and $\varrho\sigma^3 = 9$ as obtained by conventional MC and LMC. During the simulation, the system was in a cluster fcc phase. This can be seen from the pronounced peaks in the LMC data. The clustering phenomenon is reflected in the peak at $r = 0$.

#### 3. *Discretisation errors*

By discretising the simulation cell as outlined in Sec. IV A 1, we introduce two new errors to the determination of properties such as the pressure or the potential energy of the system. These errors are additional to the statistical error which is inherent to the conventional MC simulations. The first error is a structural defect, which will be dominant in case the underlying grid is not sufficiently fine, as the use of a lattice introduces anisotropies. However, the Shannon-Nyquist sampling theorem tells us that discrete samples are a complete representation of the original property if we choose the lattice discretisation parameter sufficiently large so that all relevant frequencies of the structure factor of the system (which is proportional to the Fourier transform of the RDF) are captured. If this condition is fulfilled, the sampling of the structure of the system (i.e., the measurement of the RDF) is fine enough to not lose any information [15].

The other error is due to linearisation. Resulting from the presence of the grid, we do obtain particle positions that are no longer uniformly distributed in $[0, L) \times [0, L) \times [0, L)$ but rather form a set of discrete positions $\{x_i, y_j, z_k\}$, with $i, j, k = 0, \ldots, J$, $J$ being the amount of available grid points per direction. This can be interpreted that all possible positions in the volume $\{[x_i - \delta/2, x_i + \delta/2) \times [y_j - \delta/2, y_j + \delta/2) \times [z_k - \delta/2, z_k + \delta/2)\}$ will be compared with the Boltzmann distribution at $\{x_i, y_j, z_k\}$. Taking averages of a property $A$, only the function values $A(x_i, y_j, z_k)$ are used. Therefore, integrals in LMC simulations are reduced to a (Riemann) sum over all grid sites. Thus, we can conclude that the linearisation error scales the same way as Riemann sums scale, i.e. with $J^{-2}$. It has to be stressed that even when performing an LMC simulation of *infinite* length, the end result would still be afflicted with this linearisation error since the discretisation of the grid remains fixed throughout the simulation.

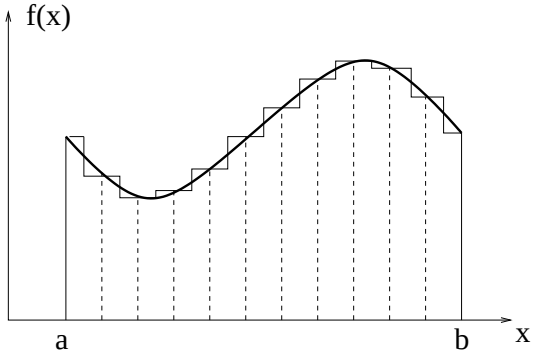


FIG. 7: One-dimensional representation of an integration in the LMC scheme. Since only the discrete positions of the grid (dashed lines) are allowed in interval [a,b], the MC summation converges towards the Riemann sum and not the integral anymore.

### B. Cell Lists

To speed-up simulations of systems with a large number of particles, Quentrec and Brot [16] developed the so called cell list method. The cubic simulation cell is divided into $M \times M \times M$ sub-cells with a size $r_m = L/M$ greater than the range of the potential. A two dimensional representation of this idea is shown in Fig. 8. Therefore, each particle in a given cell only interacts with particles in the same or in the surrounding cells. Using this method, we only need to consider $27NN_m$ pairs of particles, where $N_m = N/M^3$ is the average number of particles per cell, instead of $\frac{1}{2}N(N-1)$ (cf. Sec. III).

To realise this method, linked lists can be used [7]. First, all particles have to be assigned to their respective cells, which is a rapid process. In an array called "head-of-chain", the identification number of one particle of each cell is stored. This number is then used to address the element of a linked list array, which contains

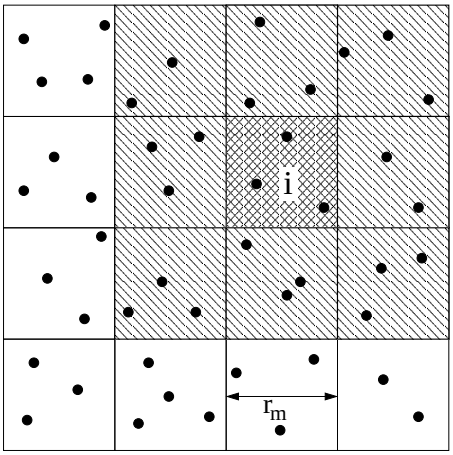


FIG. 8: Schematic representation of the cell list method in two dimensions: the simulation box is divided into $M \times M$ cells of length $r_m$. A particle in cell $i$ interacts only with all particles of its cell or of the neighbouring cells (simply shaded cells).

the identification number of the next particle in the cell. In turn, the array element for this particle is the index of the next one, and so forth. Via this method, one can address all the particles in a cell until the element 'zero' is reached, which signals the end of the list. Then, one has to move on to the head of chain of the next cell. After each accepted MC move, there is the possibility that the moved particle has left its cell. At the cost of some extra book-keeping, the time-consuming creation of a new list after every accepted move can be avoided and the existing linked list can be updated instead.

## V. RESULTS

First, we want to study the influence of the lattice discretisation parameter $\zeta$, which is controlled by the number of bits used, on the structural properties in a qualitative way. Fig. 9 shows three simulation snapshots of a GEM-4 at $\varrho\sigma^3 = 9$ and $\beta\varepsilon = 1$ (for the location of this state cf. the phase diagram in Fig.14). The upper left panel shows the system at $b = 5$. In each direction, there are only 32 positions available, which strongly influences the structure of the system. The same system is shown for a grid at $b = 6$ (upper right panel). Now, the structure is already reproduced in a more appropriate way, though the effects of the grid can still easily be seen. At $b = 8$ (lower panel), the discretisation is sufficiently fine to guarantee reliable results on the structure.

In Fig. 10 we show the structure in a more quantitative way by studying the RDF within the same system. We see that already at a discretisation of 6 bits per direction, we get qualitative agreement with the data from conventional MC simulations. At 8 bits, all the characteristic features of the RDF are captured. It has to be stressed

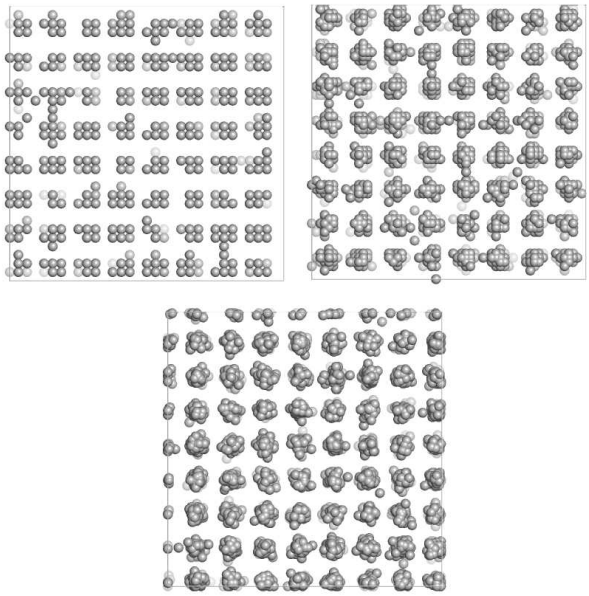

FIG. 9: Snapshots from LMC simulations of a GEM-4 system at $\varrho\sigma^3 = 9$ and $\beta\varepsilon = 1$ for discretisations of $b = 5$ (upper left), 6 (upper right), and 8 (lower panel). Different shades are used to adumbrate the third dimension.

that the data presented are from a system frozen into a face centered cubic (fcc) crystal. In this case, the RDF measured during the LMC simulation will exhibit very distinct peaks at certain distances (cf. Fig. 6), while the data presented in Fig. 10 have already been smoothed. As it can be seen in Fig. 11, in the fluid state the data for the RDF shows less fluctuations.

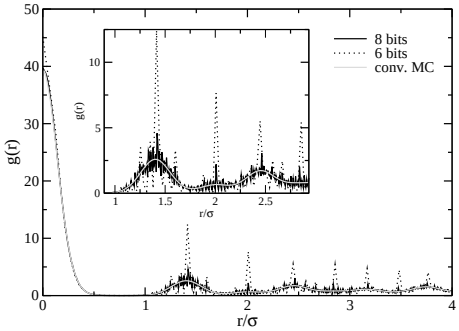


FIG. 10: The radial distribution function for a GEM-4 system at $\varrho\sigma^3 = 9$ and $\beta\varepsilon = 1$ and frozen into a cluster fcc crystal for LMC simulations at $b = 6$ and 8 and compared to conventional MC simulation results.

We conclude the discussion of structural properties by showing a radial distribution function for the centers of mass of the clusters (instead of the particles themselves) in Fig. 12. It can be seen that already at very low values of $b$, we obtain qualitatively correct results. The curves of $b = 7$, 8, and 9 coincide and reproduce the data of

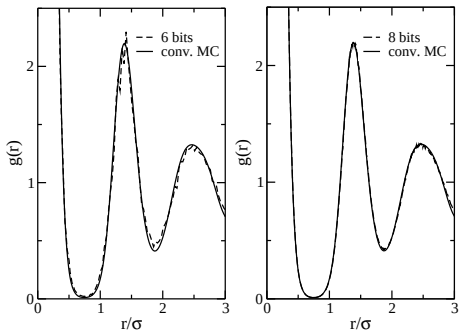


FIG. 11: The radial distribution function for a GEM-4 system at $\varrho\sigma^3 = 9$ and $\beta\varepsilon = 1$ in a supercooled liquid configuration for LMC simulations at $b = 6$ (left) and $b = 8$ (right) in comparison with conventional MC simulation results.

conventional MC perfectly.

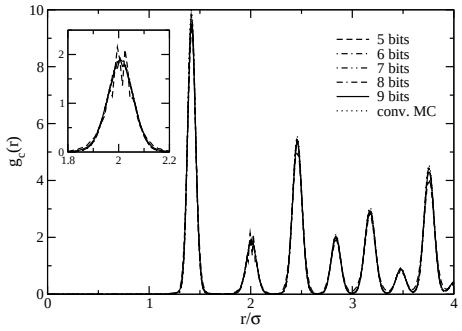


FIG. 12: The radial distribution function for the centres of mass of a GEM-4 system at $\varrho\sigma^3 = 9$ and $\beta\varepsilon = 1$ as obtained by LMC simulations at different levels of discretisation and compared to results of conventional MC simulations.

Even though the results of the structural properties might suffer from small fluctuations, the situation is different for the *thermodynamic* properties, such as the pressure or the internal energy. They are calculated as ensemble averages and hence are not affected by the small deficiencies observed in the structural properties. From our results for different levels of discretisation and by comparing them to the results of the conventional MC approach, we conclude that 8 bits are sufficient to gather the required numerical accuracy in the structural and the thermodynamic properties. We want to stress that higher levels of discretisation go along with a considerably larger demand in memory, since the size of the array that stores all the possible interactions scales as $2^{2(b-1)}$ (cf. Sec. IV A 1). Moreover, for these levels of discretisation, also considerably increased array access times have to be taken into account.

In case of the GEM-$n$, the LMC technique and the use of cell lists result in an average speed up of 15. This has brought extensive quantitative studies of the GEM-$n$ within reach. In our studies, we concentrated on the GEM-4 to analyse the clustering phenomenon in general. The main aim of this study was to determine the phase behaviour of the system. Supplementing the MC results with liquid state and density functional theory (DFT) calculations, we were able to calculate the free energies $F$ of the different phases (see Fig. 13) and to draw the phase diagram (see Fig. 14). As already predicted in Ref. [1], the system freezes at every temperature into a cluster solid. The preferred structure at high densities is the fcc structure. Above the triple temperature $(\beta\varepsilon)^{-1} \sim 0.4$, a wedge shaped region of a body centered cubic (bcc) cluster solid emerges between the liquid and the fcc phase of the cluster solid. The details of this can be found in Ref. [17].

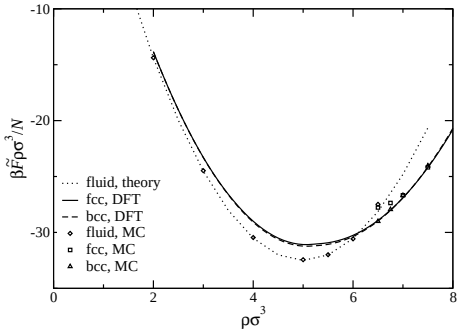


FIG. 13: Modified free energy density $\beta\tilde{F}\varrho\sigma^3/N = \beta F\varrho\sigma^3/N + K_1\varrho\sigma^3$ according to LMC simulations and liquid state and density functional theory calculations as a function of the density at $\beta\varepsilon = 1$ for the GEM-4 model. A term linear in density was added for clarity, with $K_1$ being an irrelevant constant. The error bars of the LMC simulations are smaller than the symbol sizes.

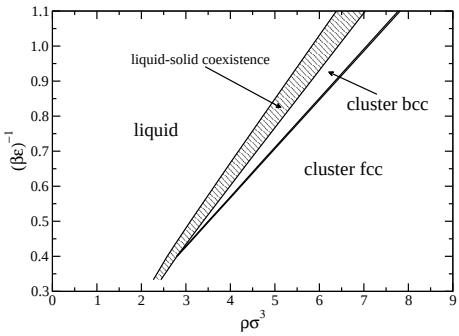


FIG. 14: Phase diagram of the GEM-4 model.

## VI. CONCLUSION

We studied a novel mechanism of cluster formation in purely repulsive potentials. To reliably analyse the behaviour of the system within MC simulations, sufficiently large systems have to be studied. Conventional

MC simulations suffer from inefficiently long simulations times. However, by implementing a lattice Monte Carlo method, where particles are just allowed to move on a fine grid, and combining it with cell lists, extensive simulations become feasible without loosing accuracy in the results. Thus, it was possible to study the system in detail and to obtain a quantitative description of the phase diagram [17].

## VII. ACKNOWLEDGEMENTS

This work was carried out within a collaboration with Daan Frenkel and Josep C. Pàmies at AMOLF in Amsterdam. I would like to thank both of them for useful discussions and their assistance in my work. I also would like to thank Laura Leistikow, Willem Vermin, and Bert van Corler for their hospitality and their assistance with the use of the supercomputers at SARA. Apart from that, I am indebted to Dieter Gottwald, Gerhard Kahl, Christos N. Likos, and Martin Neumann for their indispensable contributions to this project. The work was carried out under the Project HPC-EUROPA (RII3-CT-2003-506079), with the support of the European Community - Research Infrastructure Action under the FP6 "Structuring the European Research Area" Programme. It was also supported by the Austrian Science Fund FWF, Project Nos. P15758 and P17823.

[1] C. N. Likos, Phys. Rep. **348**, 267 (2001).
[2] W. B. Russel, D. A. Saville, and W. R. Schowalter, *Colloidal Dispersions* (Cambridge, 1990).
[3] J. Hafner, *From Hamiltonians to Phase Diagrams* (Springer Verlag, Berlin, 1987).
[4] C. N. Likos, H. Löwen, M. Watzlawek, B. Abbas, O. Jucknischke, J. Allgaier, and D. Richter, Phys. Rev. Lett. **80**, 4450 (1998).
[5] A. A. Louis, P. G. Bolhuis, J. P. Hansen, and E. J. Meijer, Phys. Rev. Lett. **85**, 2522 (2000).
[6] I. O. Götze, H. M. Harreis, and C. N. Likos, J. Chem. Phys. **120**, 7761 (2004).
[7] D. Frenkel and B. Smit, *Understanding Molecular Simulation* (Academic Press, London, 2002), 2nd edition.
[8] C. N. Likos, A. Lang, M. Watzlawek, and H. Löwen, Phys. Rev. E **63**, 031206 (2001).
[9] D. Gottwald, C. N. Likos, G. Kahl, and H. Löwen, Phys. Rev. Lett. **92**, 068301 (2004).
[10] D. Frenkel, see link `http://www.bell-labs.com/jc-cond-mat/june/jccm_jun04_03.html`
[11] B. M. Mladek, *Integral Equation Theories and Computer Simulations for Systems with Bounded Potentials* (diploma thesis, see link `http://tph.tuwien.ac.at/smt/Mladek/diplomarbeit.pdf`, 2003).
[12] B. M. Mladek, C. N. Likos, G. Kahl, and M. Neumann, unpublished.
[13] A. Z. Panagiotopoulos, J. Chem. Phys. **112**, 7132 (2000).
[14] J. P. Hansen and I. R. McDonald, *Theory of Simple Liquids* (Academic Press, London, 1986), 2nd edition.
[15] H. Fragner, *Lattice Monte Carlo Simulationen mit rekonfigurierbaren Prozessoren* (PhD thesis, Universität Wien, 2005).
[16] B. Quentrec and C. Brot, J. Comput. Phys. **13**, 430 (1975).
[17] B. M Mladek, D. Gottwald, G. Kahl, M. Neumann, and C. N. Likos, Phys. Rev. Lett. **96**, 045701 (2006).